

# Minimizing Tool Wear, Cutting Temperature and Surface Roughness in the Intermittent Turning of AISI D3 Steel Using the DF and GRA Method

Fethi Khelfaoui<sup>a</sup>, Mohammed Athmane Yallese<sup>a</sup>, Septi Boucherit<sup>a,\*</sup>, Hanane Boumaaza<sup>b</sup>, Nourdine Ouelaa<sup>a</sup>

<sup>a</sup>Laboratory of Mechanics and Structure (LMS), Department of Mechanical Engineering, University 8 May 1945, P.O. Box 401, 24000 Guelma, Algeria,

<sup>b</sup>Laboratory of Applied Mechanics and New Materials (LAMNM), Department of Mechanical Engineering, University 8 May 1945, P.O. Box 401, 24000 Guelma, Algeria.

## Keywords:

Intermittent turning  
AISI D3  
RSM  
Modeling  
GRA

\* Corresponding author:

Septi Boucherit   
E-mail:  
[Boucherit.sebti@univ-guelma.dz](mailto:Boucherit.sebti@univ-guelma.dz)

Received: 30 October 2022

Revised: 21 November 2022

Accepted: 3 January 2023

## ABSTRACT

Intermittent turning (IT) is characterized by a different context than continuous turning (CT). The cutting tool is shocked each time it goes off-load and engages a new surface. This interruption causes severe cutting conditions, which fatally affect the performance parameters. The purpose of this study is to assess the effects of four cutting factors, tool nose radius ( $r$ ), cutting speed ( $V_c$ ), feed rate ( $f$ ), and depth of cut ( $a_p$ ), on the following output performance parameters: surface roughness ( $R_a$ ), cutting temperature ( $T^\circ$ ), and cutting tool wear ( $V_B$ ) during turning (IT) AISI D3 cold work tool steel. A triple CVD ( $Al_2O_3/TiC/TiCN$ )-coated carbide cutting tool was used. A Taguchi L9 ( $3^4$ ) experimental design was adopted for carrying out the experiments in intermittent turning. To improve the performance parameters based on three (3) highly particular scenarios that fulfill industrial criteria, the desirability function (DF) and the grey relational analysis method (GRA) were used. Finally, the optimization findings of the two strategies were compared in order to evaluate the performance of each method.

© 2023 Published by Faculty of Engineering

## 1. INTRODUCTION

The correct choice of the cutting parameters of a machining operation is very important to achieve industrial objectives, but it is first necessary to have knowledge of the machining context, the material being machined, as well as the cutting tool used [1]. Intermittent turning is a

complicated operation due to the consequences created by the cut's discontinuity. Shocks generated by the cutting tool have a significant impact on its performance characteristics. During intermittent machining, tool wear and cutting temperature must be regulated due to their detrimental influence on the cutting tool, both directly and indirectly, on the surface

quality of the machined parts [2]. For evaluating the impact of input parameters on outputs, modeling and optimization approaches are crucial and very successful. Several papers have been published on the intermittent turning of (AISI D3) and the modeling and optimization of cutting parameters. In this context of machining (IT), several research studies have been carried out. Ko et al. [3] carried out a study on the intermittent hard turning of bearing steel (AISI 52100) in order to evaluate the performance of cutting tools (CBN) with different nitride contents. The output factors ( $V_B$ ), (Ra), and (Fz) were monitored. The results prove that increasing the nitride content induces a decrease in both Ra and  $V_B$  and that the cutting force reduces as the cutting speed increases. This is because the increased cutting temperature softens the workpiece. Liu et al. [4] conducted experiments in (IT) using two different cutting tools (YT5 and GC4235) on high-strength steel 2.25Cr1Mo0.25V. The results obtained showed that at low cutting speeds, the predominant wear form of cemented carbide YT5 is flank wear, but at high cutting speeds, the predominant wear form is breakage, and tool life is limited. In addition, the study revealed that the performance of the tool (GC4235) is superior to that of the tool (YT5). The cutting performance of a quadrate (GC4235) coated carbide tool in IT of 2.25Cr1Mo0.25V material was investigated by Liu et al. [5]. There have been proposed empirical models of the parameters (MRR) and (Fz) as a function of the factors ( $V_c$ ), ( $a_p$ ), and ( $f$ ). Abrasive wear and chipping were also the predominant wear mechanisms at low cutting speeds. On the other hand, when cutting at high speeds, coatings often peel off and adhesives break down. Vibration-based (IT) experiments were conducted by Carou et al. [6]. The effect of vibrations on the feed rate, minimum quantity lubrication (MQL) flow rate, and workpiece interruption type is investigated. The findings shows that part of the vibrations depend on the MQL system's flow rate and feed rate interaction, not the interruption type. The MQL system has more impact at lower feed rates. Vibrations strongly affect surface roughness. This relationship varies by environment. Under dry circumstances, surface roughness increases with vibrations, but the MQL system reverses this. Gong et al. [7] investigated the (IT) of 20CrMnTi tempered steel using an  $Al_2O_3$ -TiC ceramic. The cutting forces and failure mechanisms of the

cutting tools were investigated as the cutting conditions varied. The findings showed that as tool wear increased, the effect of cutting parameters on cutting forces decreased while the contribution of depth of cut to cutting forces increased. Cui et al. [8] used an  $Al_2O_3$ /(W, TiC) ceramic cutting tool to investigate the optimal cutting parameters in the (IT) of AISI 1045 steel. Using FEM as an optimization approach, the findings obtained allowed for an ideal area of surface roughness, cutting energy, and specific energy consumption. Recently, Kudryashova et al. [9] conducted an experimental study in (IT), in order to understand the stabilization of cutting tools on complex surfaces. The analysis of the results showed that (Ra) is improved by 20% to 70% if a tool equipped with a damping element in the (IT) replaces the standard tool. Also, Nayak et al. [10] performed a comparison between the (CT) and (IT) of AISI D6 tool steel using a low CBN tool. The results found in (IT) show that  $V_c$  does not affect the cutting forces, and the wear mechanisms are abrasion and diffusion. On the other hand, high-alloy steel (AISI D3) has been the subject of several experimental studies that focus on machinability, MQL lubrication, tool wear, modelling, and optimization of cutting conditions. [11–13]. The desirability function (DF) and the grey relational analysis method (GRA) are two methods widely used by many researchers because of their simplicity, efficiency, and other advantages [14–16]. The review of the previous literature clearly shows that intermittent turning presents a case study frequently encountered in the industry, and this particular case of machining deserves special attention in order to evaluate, model, and optimize the technological performance parameters in this machining context. Also, the particularity of this work lies in the fact that little investigation has been carried out on the (IT) of AISI D3 steel by considering the particular intermittent form on the workpiece and by considering four factors of input and three factors of output technical characteristics. Add to this a comparison of the optimal cutting regimes obtained by two distinct optimization methods. The aim of this study is to analyze the performance parameters (Ra,  $T^\circ$ , and  $V_B$ ) in relation to the cutting conditions ( $r$ ,  $V_c$ ,  $f$ , and  $a_p$ ) during (IT) of AISI D3 steel. ANOVA was used to quantify the impact of input variables on responses. Statistical analysis of the results allowed the development of prediction models in

the context of (IT). A multi-objective optimization of cutting variables was performed using two techniques: (DF) and (GRA). Finally, a comparison of the results was made.

## 2. EXPERIMENTAL PROCEDURE

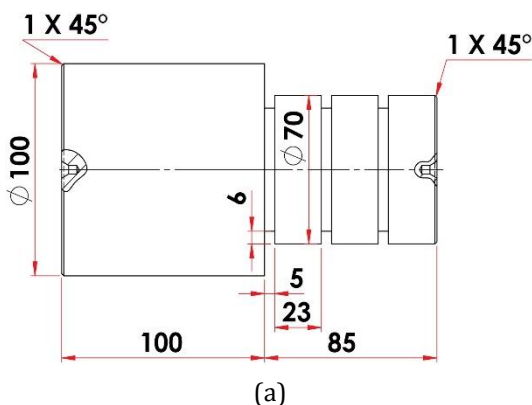
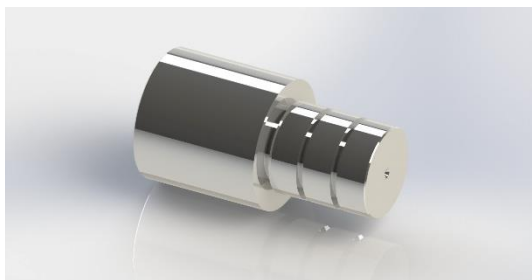
### 2.1 Cutting tool and workpiece

The specimen material used in the experiments is high-alloy steel (AISI D3) suitable for cold working. The specimen is 185 mm long and 70 mm in diameter, mounted on the machine in mixed assembly. In order to ensure intermittent turning, three equal 23 mm bearings were made, separated by three 5 mm wide grooves over a machining length of 85 mm (Fig. 1a). A triple-coated metal carbide insert (Al<sub>2</sub>O<sub>3</sub>/TiC/TiCN) of Sandvik designation (GC4215) was used (Fig. 1b). The workpiece was held in place by a designation tool holder (PSBNR 2525M 12) with a common active part tool geometry described by  $\chi_r = +75^\circ$ ,  $\alpha_c = +6^\circ$ ,  $\gamma = -6^\circ$ ,  $\lambda = -6^\circ$ ,  $H = 25\text{ mm}$ ,  $B = 25\text{ mm}$  (Fig. 1c).

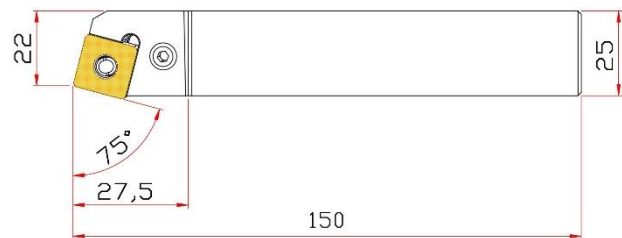
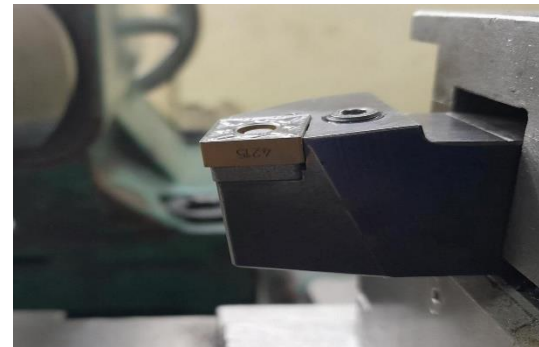
In intermittent machining, each cutting edge is subjected to three (03) impacts in succession.

**Table 1.** AISI D3 chemical composition (in percent).

C	Si	Ni	Mo	Mn	S	P	Cu	Cr
2	0.3	0.25	0.12	0.29	0.009	0.011	0.16	12



(b)



(c)

**Fig. 1.** (a) Workpiece, (b) Cutting insert and (c) Tool holder.

### 2.2 Plan of experiments and measuring equipment

A Taguchi L9 (3<sup>4</sup>) design was used in order to reduce the number of tests and consequently minimize the cost and time of the experiments. The intermittent turning tests were performed on a Tos Trencin (SN40C) lathe with a power of 6.6 KVA. Surface roughness (Ra) was measured at three angular points of 120° for each test using an MITUTOYO SJ-210 roughness meter. The average of the three measurements was taken into consideration in the results (Fig. 2a).

The temperature (T°) was measured in real time by a Raycam CA 1884 I.R. thermography camera during the machining operation. The temperature considered in this work was measured at the end of the machining of the three bearings. The camera was positioned 300 mm from the cutting area and fixed to a rigid support at 45°. The emissivity was

set to (0.9) on a scale of (0.01–1); this corresponds to the emissivity of the machined material. The thermal camera displays the maximum temperature in the cutting area (Fig. 2b).

The wear ( $V_B$ ) on the tool's clearance surface was measured at the end of the machining of the three bearings using a VISUEL GAGE 250 microscope (Fig. 2c). For each test in Table (3), a new cutting edge was used. Table (2) summarizes all the operating conditions used, and Figure (2) shows the experimental procedure in (IT). The values of the cutting conditions ( $r$ ,  $V_c$ ,  $f$ , and  $a_p$ ) were chosen according to the recommendations of the tool manufacturer (Sandvik) and based on the concept of the tool/material pair (according to ISO 3685).

**Table 2.** Operating conditions of the experiments

Elements	Description
Lathe	SN40C (6.6 KVA)
workpiece	AISI D3
Cutting speed	240 ; 280; 320 m/min
Feed rate	0.08 ; 0.12 ; 0.16 mm/rev
Depth of cut	0.3 ; 0.6 ; 0.9 mm
Nose raduis	0.4 ; 1.2 ; 1.6 mm
Cutting environment	Dry intermittent turning
Cutting tool	(CVD)Carbide insert coating $Al_2O_3+TiC$ TiNC
Tool holder	SANDVIK PSBNR 2525M 12
Responses	$R_a$ ( $\mu m$ ) ; $T^\circ$ ( $^\circ C$ ) ; $V_B$ (mm)

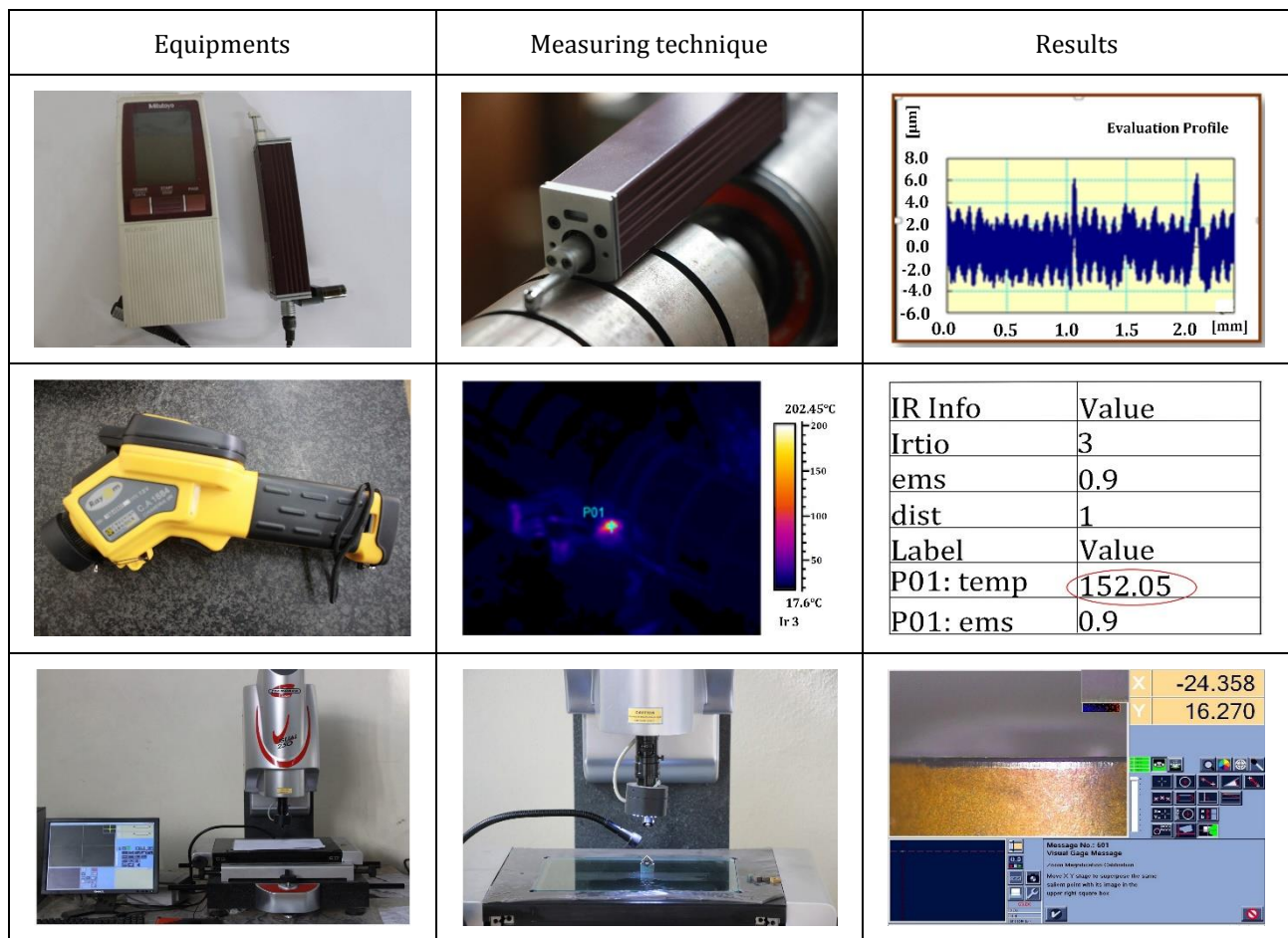


**Fig. 2.** Experimental procedure and measuring equipments.

### 3. RESULTS AND DISCUSSION

#### 3.1 Experimental results

Table (3) presents the results of the tests carried out, showing the values of the response parameters ( $R_a$ ), ( $T^\circ$ ) and ( $V_B$ ) as a

function of the variation of the input factors ( $r$ ), ( $V_c$ ), ( $f$ ), and ( $a_p$ ) during intermittent turning. An analysis of the results shows that the output parameters vary as follows: ( $R_a$ ) ranges between 0.825  $\mu m$  and 1.201  $\mu m$ , ( $T^\circ$ ) between 198  $^\circ C$  and 235  $^\circ C$  and that ( $V_B$ ) is between 0.064mm and 0.074 mm.

**Table 3.** Experimental results.

EXP N°	Input factors				Output factors		
	r	Vc	f	ap	Ra	T°	V <sub>B</sub>
1	0.4	240	0.08	0.3	0.867	198	0.064
2	0.4	280	0.12	0.6	1.034	220	0.070
3	0.4	320	0.16	0.9	1.201	235	0.074
4	1.2	240	0.12	0.9	0.934	225	0.068
5	1.2	280	0.16	0.3	1.060	223	0.071
6	1.2	320	0.08	0.6	0.873	224	0.070
7	1.6	240	0.16	0.6	0.938	226	0.068
8	1.6	280	0.08	0.9	0.825	228	0.069
9	1.6	320	0.12	0.3	0.878	229	0.072

### 3.2 ANOVA for (Ra, T° and V<sub>B</sub>)

ANOVA is a method for exploring and assessing the relationship between a performance metric and one or more technological influencing factors. The probability value (p) represents the effect of each parameter. The factor is significant if it is greater than 0.05 ( $p > 0.05$ ). If p is less than 0.05, the factor is deemed negligible [17]. The ANOVA findings for the responses (Ra, T°, and V<sub>B</sub>) are shown in Table 4. The (Ra) ANOVA reveals that the variables (f) and (r) have a significant impact, with cont% of 57.86% and 29.63%, respectively. The factor (Vc) is likewise important, with a cont% of 6.53%, whereas the factor (ap) is not, with a cont% of 3.46%. The findings support previous findings in the literature about the predominance of (f) over (Ra) [18,19]. Temperature (T°) ANOVA clearly reveals that all input variables are significant. The factors (Vc) and (ap) have the greatest influence on (T°). This is due to the fact that the heat source comes from the plastic deformations, which increase with the increase in the section of the chip (fxap), and also from the friction, which is more pronounced with the increase in speed. In addition, friction increases with increasing insert nose radii since the contact length between the cutting edge and the workpiece increases. Their respective contr% are 29.72% and 28.22%. The factor (f) ranks third with a cont% of 22.59%, whereas (r) ranks lower with a cont% of 17.98%. Similar findings have been reported in the literature, demonstrating that the variables (Vc) and (ap) are the primary causes of the rise in (T°) [20,21]. The ANOVA of (V<sub>B</sub>) shows that the factors (Vc) and (f) have the greatest influence on (V<sub>B</sub>) with cont% of 66.44% and 25.95%, respectively, because, in addition to the increase in temperature in the cutting zone, the increase in friction promotes wear by abrasion, as shown in Figure 3 by the streaks on the strip of flank wear, while the

factors (r) and (ap) are insignificant with P-values of 0.565 and 0.083. These results are in perfect agreement with those of [22].

**Table 4.** ANOVA of Ra, T° and V<sub>B</sub>.

Source	DF	Cont %	CM ajust	F-Values	P-Values
<b>ANOVA of Ra</b>					
r	1	29.63%	0.034304	46.96	0.002
vc	1	6.53%	0.007561	10.35	0.032
f	1	57.86%	0.066993	91.70	0.001
ap	1	3.46%	0.004004	5.48	0.079
Error	4	2.52%	0.000731		
Total	8	100.00%			
<b>ANOVA of T°</b>					
r	1	17.98%	153.341	48.24	0.002
vc	1	29.72%	253.5	79.75	0.001
f	1	22.59%	192.667	60.61	0.001
ap	1	28.22%	240.667	75.72	0.001
Error	4	1.49%	3.179		
Total	8	100.00%			
<b>ANOVA of V<sub>B</sub></b>					
r	1	0,31%	0	0.39	0.565
vc	1	66.44%	0.000043	84.33	0.001
f	1	25.95%	0.000017	32.94	0.005
ap	1	4.15%	0.000003	5.27	0.083
Error	4	3.15%	0.000001		
Total	8	100,00%			

Figure 3 (a, b and c) depicts the cutting tool's clearance (V<sub>B</sub>) and crater (KT) wear for the first three tests (Table 3). It is observed that the cutting conditions (Vc, f, and ap) vary from test to test, resulting in variable wear values (V<sub>B</sub>). According to the wear morphology (V<sub>B</sub>) study, the flank wear is defined by a regular band that is striped and bright. These streaks are caused by heavy abrasive wear [23]. The greater the value of the cutting conditions (Vc, f, and ap), the greater the value of the wear (V<sub>B</sub>). It is also obvious that crater wear (KT) is essentially nonexistent. Figure 4 (a, b and c) depicts the chip's morphology for testes 1, 2, and 3. It should be noted that the cutting conditions (Vc, f, and ap) have a significant impact on the form of the chip produced. Cutting conditions for tests 2 and 3 result in completely fragmented chips.

Figure 5 presents the graphs of the main effects of the output parameters (Ra), (T°), and (V<sub>B</sub>) as a function of the variations of the input factors (r), (Vc), (f), and (ap). It is noted that the factor with the greatest slope has the greatest influence on the parameter studied.

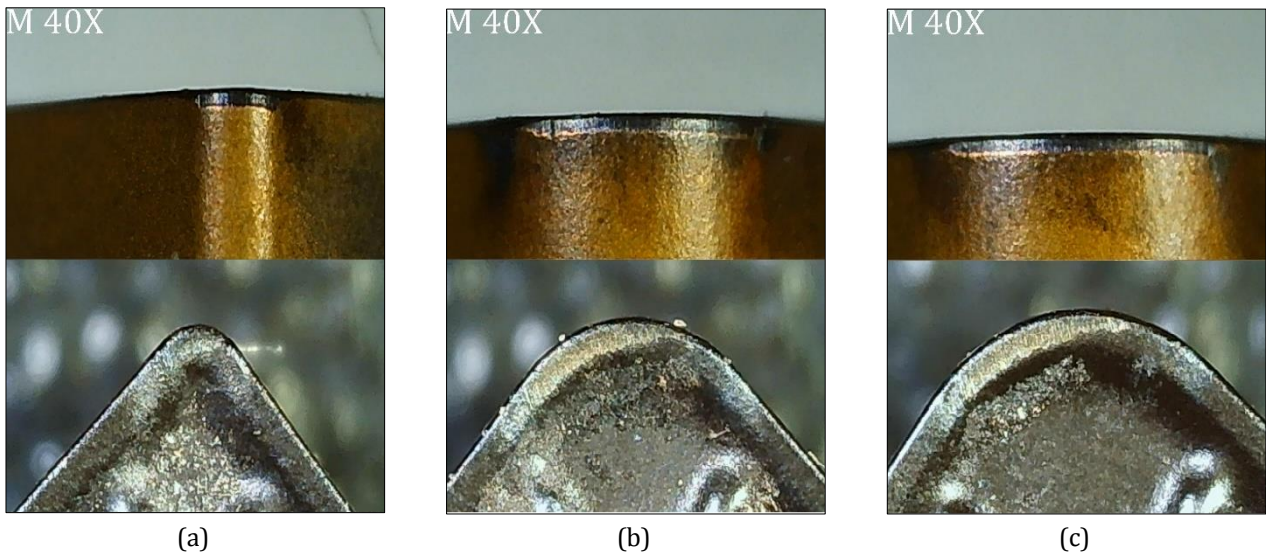


Fig. 3. Wear on the flank surface and the tool rake surface for tests 1, 2 and 3.

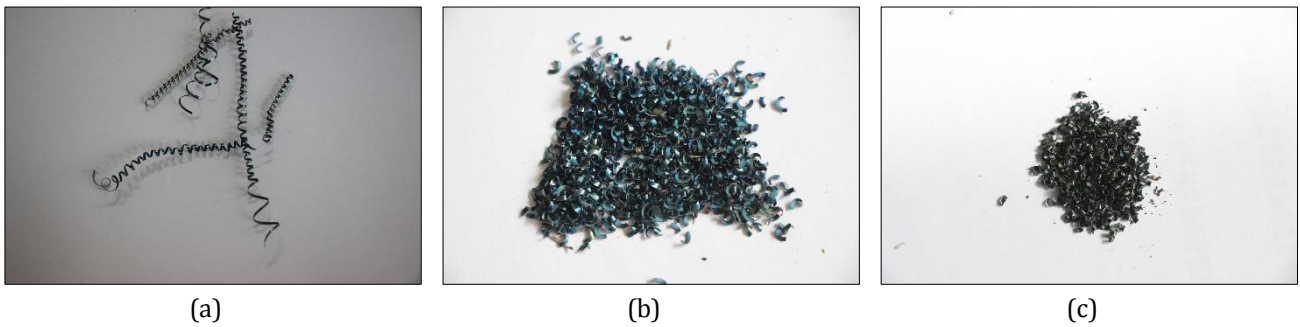


Fig. 4. Chip morphology.

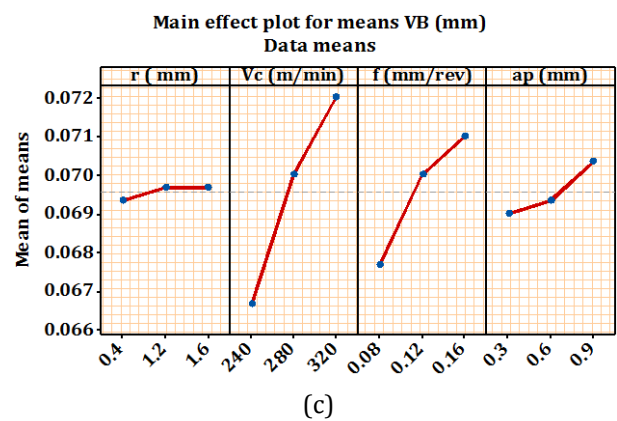
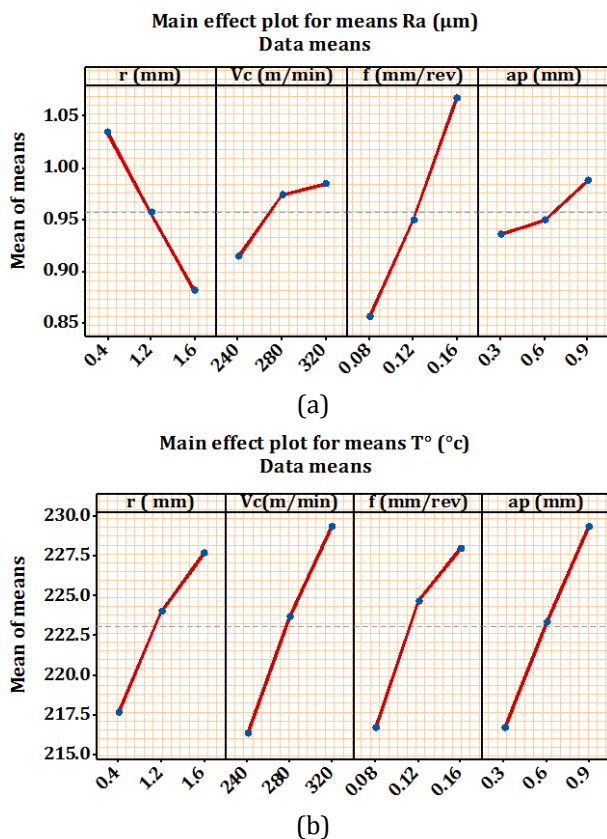


Fig. 5. Main effects graphs for ( $R_a$ ), ( $T^\circ$ ), and ( $V_B$ ).

### 3.3 Response modelling

The modelling of the performance factors of a machining operation is an important asset for prediction [23]. Linear regression equations were used to set up the statistical models (Eqs. 1-3), which show the relationship between the performance parameters ( $R_a$ ,  $T^\circ$ , and  $V_B$ ) and the input factors ( $r$ ,  $V_c$ ,  $f$ , and  $a_p$ ) in the case of intermittent machining.

$$Ra = 0.4715 - 0.1238 r + 0.000888 Vc + 2.642 f + 0.0861 ap \quad (1)$$

$(R^2 = 97.48)$

$$T^\circ = 139.12 + 8.27 r + 0.1625 Vc + 141.7 f + 21.11 ap \quad (2)$$

$(R^2 = 98.51)$

$$V_B = 0.04424 + 0.000298 r + 0.000067 Vc + 0.04167 f + 0.0022 ap \quad (3)$$

$(R^2 = 96.85)$

Figure 6 depicts the response (3-D) surfaces of the investigated performances ( $R_a$ ,  $T^\circ$ , and  $V_B$ ) in relation to the two most important input parameters. The graphs were created using the mathematical models in Eqs. 1-3. Examination of the results clearly shows that an increase in ( $V_c$ ) and ( $ap$ ) results in an increase in ( $T^\circ$ ). This is due to friction caused by the increase of ( $V_c$ ) and elasto-plastic deformations when ( $ap$ ) increases. These results are in perfect agreement with [24]. However, the increase in ( $r$ ) results in an improvement in surface quality. This is due to the smoothing phenomenon of the machined surface that occurs when ( $r$ ) increases [25]. In contrast, the increase of ( $f$ ) results in a significant increase of ( $R_a$ ), which induces a degradation of surface quality. This is mainly due to the kinematics of the cut, because the increase in ( $f$ ) creates helical grooves due to the translation movement of the tool and the rotation of the part. The greater the feed, the wider and deeper the helical furrows [12]. Finally, it can be shown that the increase in both components ( $V_c$  and  $f$ ) leads to an increase in wear ( $V_B$ ), but the effect of ( $V_c$ ) is dominant. By increasing ( $V_c$ ), the friction between the bare surface of the tool and the workpiece as well as the leading surface and the chip increases, the cutting temperature increases, and consequently the tool wear accelerates. Similar explanations have been reported by [3,26].

In order to validate the mathematical models obtained, confirmation tests were performed for  $R_a$ ,  $T^\circ$ , and  $V_B$ . The cutting parameters adopted in the confirmation tests of (IT) and the results gathered are displayed in Table 5. The results displayed in Fig. 7 show that the predicted error varies between a maximum of 3.79% and a minimum of 2.17% for ( $R_a$ ). The same errors are found to vary between 0.83% and 0.39% for ( $T^\circ$ ) and between 1.49% and 1.38% for ( $V_B$ ). Consequently, the proposed relationships satisfactorily describe the phenomenon under consideration.

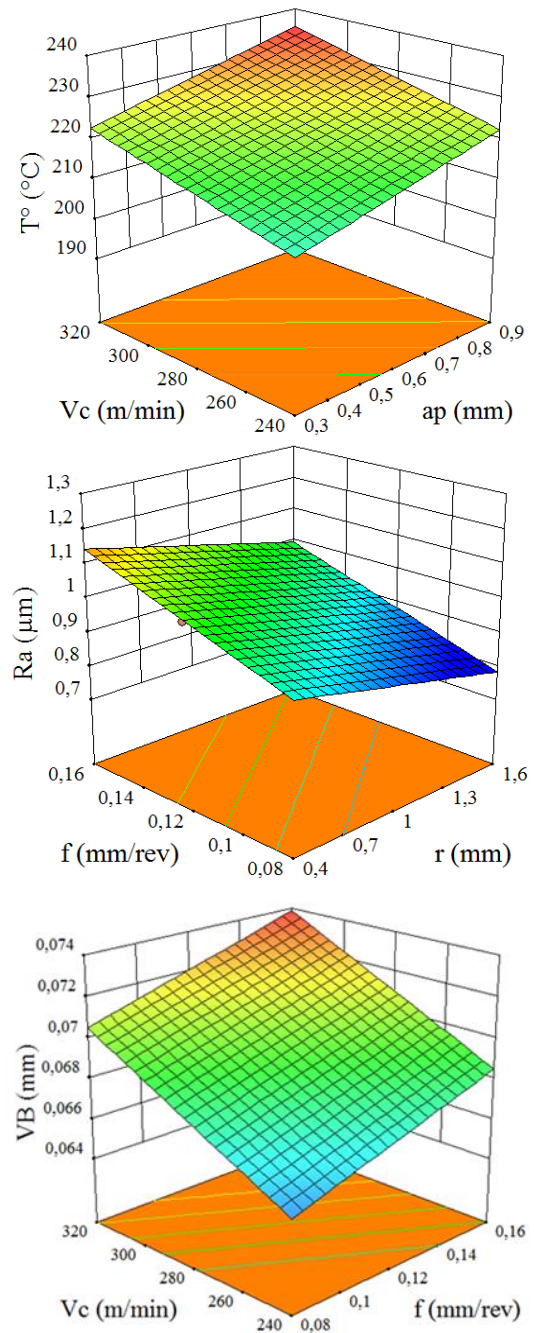


Fig. 6. Graphs (3D) of the parameters ( $R_a$ ,  $T^\circ$ ,  $V_B$ ).

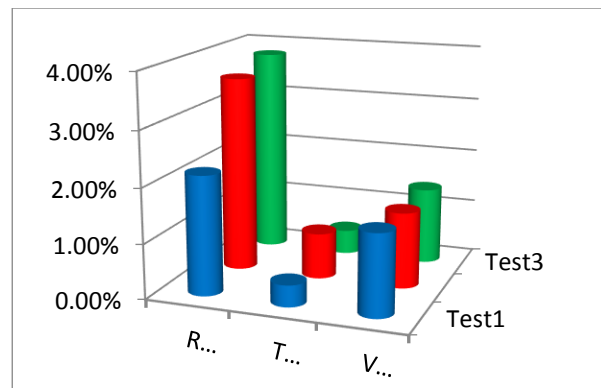


Fig. 7. Errors between predicted and experimental results.

**Table 5.** Confirmation test.

Test Number	Input factor				Output factors					
					Model Results			Test Results		
	r	Vc	f	ap	Ra	T°	V <sub>B</sub>	Ra	T°	V <sub>B</sub>
1	0.4	260	0.11	0,5	0.96011	209.403	0.067	0.981	210.23	0.068
2	1.2	300	0.14	0,7	1.01949	232.409	0.072	1.056	234.36	0.073
3	1.6	300	0.11	0,4	0.8729	232.16	0.071	0.906	233.2	0.072

**4. MULTI-OBJECTIVE OPTIMIZATION OF CUTTING PARAMETERS**

Given the process's complexity and the large number of factors investigated, multi-objective optimization is a critical asset to exploit in order to achieve industrial criteria for cost, quality, and productivity [27]. Both approaches (DF and GRA) were employed in this research to achieve this objective.

**4.1 Desirability function (DF) method**

The desirability function is exploited because of its efficiency, simplicity, and possibility to offer manufacturers several solutions in order to choose the optimal cutting parameters. Equations (4 to 6) explain the approach of (DF) [28]:

$$D(y) = \begin{cases} 0 & y < Low \\ \left(\frac{y - Low}{Tar - Low}\right)^w & Low \leq y \leq Tar \\ 1 & y > Tar \end{cases} \quad (4)$$

$$D(y) = \begin{cases} 0 & y < Low \\ \left(\frac{y - Low}{Tar - Low}\right)^w & Low \leq y \leq Tar \\ 1 & y > Tar \end{cases} \quad (5)$$

$$DF = (D_1 \times D_2 \times \dots \times D_i \times \dots \times D_n)^{\frac{1}{n}} = (\prod_{i=1}^n D_i)^{\frac{1}{n}} \quad (6)$$

Three cases of optimization are investigated in this paper. The first case involves the minimization of (Ra) as the main objective, with an importance of (5). The second case aims to minimize both (Ra) and (V<sub>B</sub>), while assigning the parameter (T°) an importance of (1). Finally, the third optimization case considers the simultaneous minimization of the three output parameters (Ra, T°, and V<sub>B</sub>) with an importance of (5). In table (6), the optimization constraints, the desired objectives, and the importance chosen for the output parameters are recorded, which varies from (1 to 5) depending on the cases studied.

Table 7 presents the first solutions proposed by the approach (DF) according to the three cases studied. Figure 8 (a, b and c) illustrates the desirability curves for the three-optimization cases.

**Table 6.** Optimization constraints and importance.

Parameters		Parameters values (V)		Objectives	Importance		
		Inf	Sup		1	2	3
Input	r	0.4	1.6	Inf ≤ V ≤ Sup	-	-	-
	Vc	240	320		-	-	-
	f	0.08	0.16		-	-	-
	ap	0.3	0.9		-	-	-
Output	Ra	0.825	1.201	Minimize	5	5	5
	T°	198	235	Minimize	1	1	5
	V <sub>B</sub>	0.064	0.074	Minimize	1	5	5

**Table 7.** Shows the solutions for three different combinations of categorical factor levels.

	r	Vc	f	ap	Ra	T°	V <sub>B</sub>	Desirability
<b>1<sup>st</sup> case</b>	0.781	240	0.08	0.30	0.825	202.250	0.064	0.976
<b>2<sup>nd</sup> case</b>	0.782	240	0.08	0.30	0.825	202.267	0.064	0.967
<b>3<sup>rd</sup> case</b>	0.781	240	0.08	0.30	0.825	202.255	0.064	0.945

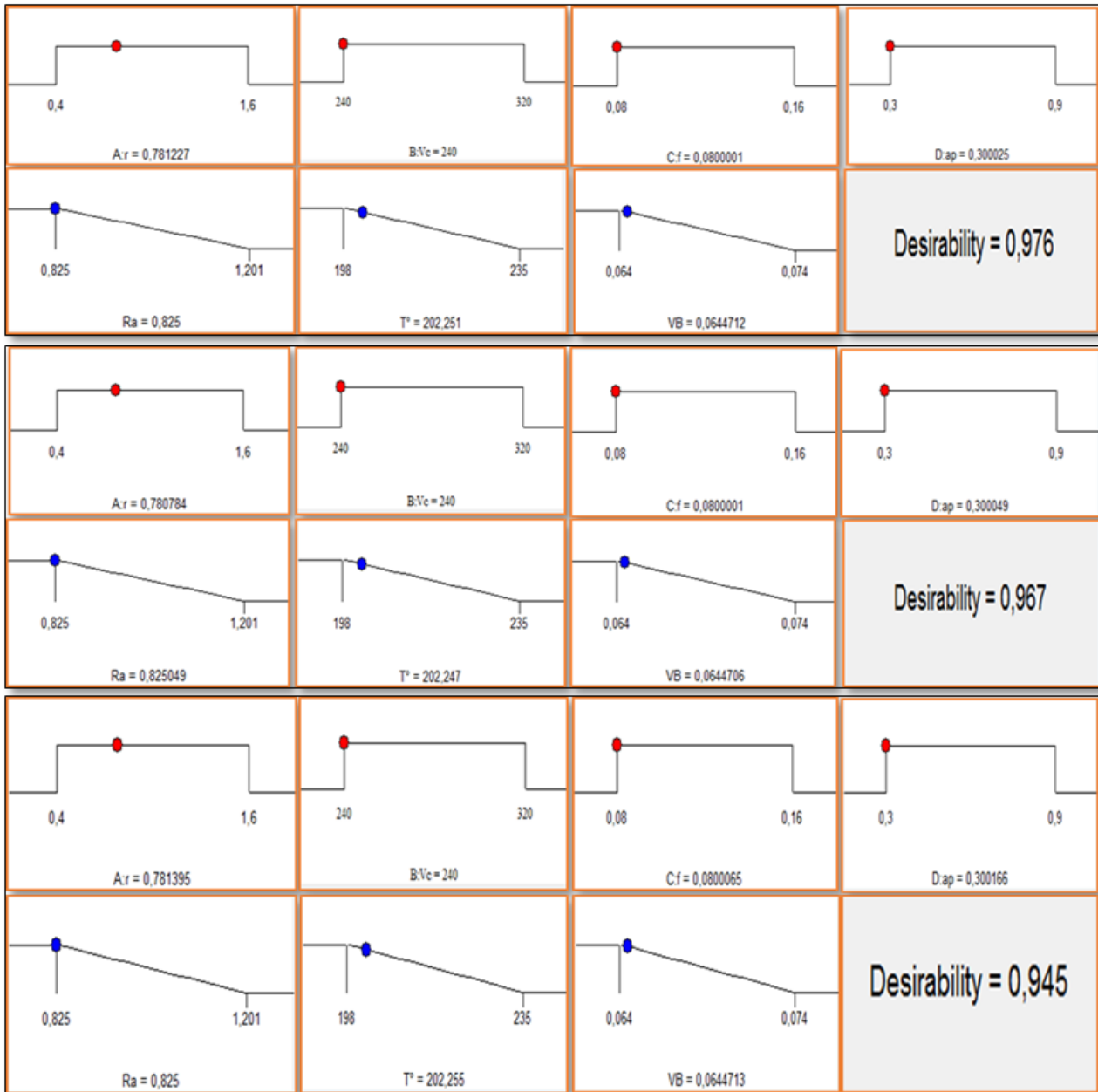


Fig. 8. Desirability ramps plots for the three optimization cases.

#### 4.2 Grey relational analysis method (GRA)

The Grey Relational Analysis (GRA) method is widely used in much research and in various fields, particularly in machining. It is effective in solving the problems of multi-objective optimization [29]. This technique is based on four steps to achieve the desired result [30].

##### Step 1: Data pre-processing

Normalization entails converting output parameters (Ra, T°, and VB) from zero to one in order to obtain quantities free of units. This step is determined by two mathematical formulas.

Smaller is better (Eq. 7); this is the case for the three output parameters (Ra, T°, and VB), i.e., the columns 2, 3, and 4 of Table 8; higher is better (Eq. 8); this case is nonexistent in this work.

$$x_i(k) = \frac{\max[y_i(k)] - y_i(k)}{\max[y_i(k)] - \min[y_i(k)]} \quad (7)$$

$$x_i(k) = \frac{y_i(k) - \min[y_i(k)]}{\max[y_i(k)] - \min[y_i(k)]} \quad (8)$$

Where:  $x_i(k)$  Normalized value;  $x_i^0(k)$  Response value;  $\max(x_i^0(k))$  Maximum value of the (k<sup>th</sup>) response  $x_i^0(k)$ ;  $\min(x_i^0(k))$  Minimum value of the (k<sup>th</sup>) response  $x_i^0(k)$

**Step 2: Grey relational coefficient**

This step consists of calculating the grey relational coefficient (GRC) after calculating the sequential deviation ( $\Delta_{0i}$ ), according to equations (9) and (10).

$$GRC = \frac{\Delta_{min} + \varphi\Delta_{max}}{\Delta_{0i}(k) + \varphi\Delta_{max}(k)} \tag{9}$$

$$\Delta_{0i}(k) = \|x_0(k) - x_i(k)\| \tag{10}$$

Where:  $\Delta_{0i}(k)$ : Deviation sequence, difference in absolute value between  $x_0^k(k)$  and  $x_i^k(k)$

$\Delta_{min}$ : The smallest value of  $\Delta_{0i}(k)$   $\Delta_{max}$ : The greatest value of  $\Delta_{0i}(k)$

$\varphi$ : Identification coefficient defined in the range  $0 \leq \varphi \leq 1$  in our case, the value of  $\beta$  is 0.5.

**Step 3: Grey relational grade**

The third step is reserved for the calculation of the grade (GRG) by equation (11). The essential factor to know in which test the optimal regime is found.

**Table 8.** Results of the GRA method.

N° EXP	Normalized value of response $x_i(k)$			deviation sequence $\Delta_{0i}(k)$			Coefficient GRC			GRG	Rank
	Ra	V <sub>B</sub>	T°	Ra	V <sub>B</sub>	T°	Ra	V <sub>B</sub>	T°		
1	0,888	1	1	0,112	0	0	0,817	1	1	<b>0,939</b>	<b>1</b>
2	0,444	0,4	0,405	0,556	0,6	0,595	0,473	0,454	0,456	0,461	7
3	0	0	0	1	1	1	0,333	0,333	0,333	0,333	9
4	0,71	0,6	0,27	0,29	0,4	0,73	0,632	0,555	0,406	0,531	4
5	0,375	0,3	0,324	0,625	0,7	0,676	0,444	0,416	0,425	0,428	8
6	0,872	0,4	0,297	0,128	0,6	0,703	0,796	0,454	0,415	0,555	3
7	0,699	0,6	0,243	0,301	0,4	0,757	0,624	0,555	0,397	0,525	5
8	1	0,5	0,189	0	0,5	0,811	1	0,5	0,381	0,627	2
9	0,859	0,2	0,162	0,141	0,8	0,838	0,78	0,384	0,373	0,512	6

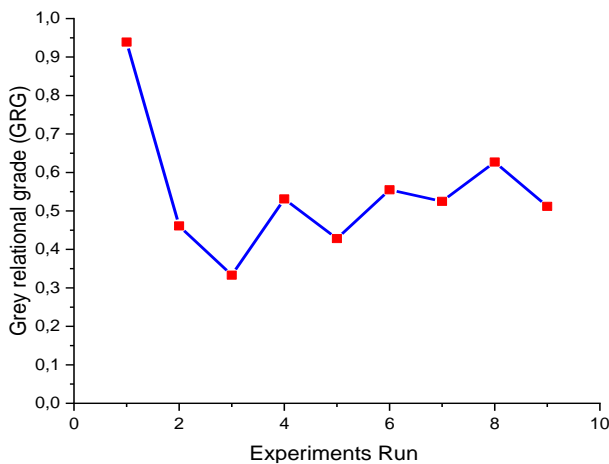


**Fig. 9.** GRG for each trial.

$$GRG = \frac{1}{n} \sum_{k=1}^n GRC \tag{11}$$

**Step 4: Confirmation test**

The last step is reserved for the confirmation test. It can be calculated by the equation (12).

$$\gamma_i = \gamma_m + \sum_{i=1}^p (\bar{\gamma}_i - \gamma_m) \tag{12}$$

Where  $\gamma_m$  is the total mean GRG,  $\bar{\gamma}_i$  is the mean GRG at the optimal level, P: is the number of major variables.

Table 8 summarizes all the results given by the GRA. It is clear that the first experiment has the highest value of GRG (0.939), which implies that the cutting conditions ( $r = 0.4$  mm,  $V_c = 240$  m/min,  $f = 0.08$  mm/rev, and  $a_p = 0.3$  mm) are the optimal parameters, which give the values of the following performance parameters  $R_a = 0.867\mu\text{m}$ ,  $V_B = 0.064$  mm, and  $T^\circ = 198$  °C. The graphical representation of (GRG) for each test is given in Figure 9, and Figure 10 presents the main effects plot, which clearly shows the optimal regime.

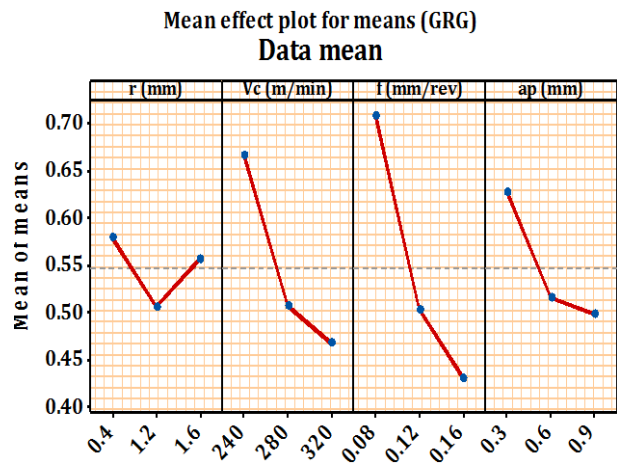


**Fig. 10.** Main effects graph.

### 4.3 Comparison between DF and GRA results

The results obtained from the application of two optimization methods are illustrated in Table 9. The analysis of the two optimal modes shows that the two methods (DF and GRA) propose the same optimal combination for the factors ( $V_c = 240$  m/min), ( $f = 0.08$  mm/rev), ( $a_p = 0.3$  mm), but a minimization of (-

48.784%) for factor ( $r$ ). Two output parameters ( $R_a$ ) and ( $T^\circ$ ) have different values, i.e., a percentage difference of (5.09%) and (-2.089%), respectively. A similar value for the factor ( $V_B$ ) is equal to (0.064 mm). Simultaneous optimization by minimizing ( $R_a$ ), ( $T^\circ$ ), and ( $V_B$ ) is ensured by the two methods, which offer manufacturers the possibility of exploiting the two proposed regimes.

**Table 9.** Results of optimization by (DF and GRA).

method	Input Parameters				Output Parameters			Decision value
	r	Vc	f	ap	Ra	T°	V <sub>B</sub>	
DF	0.781	240	0.08	0.3	0.825	202.22	0.064	0.945
GRA	0.4	240	0,08	0,3	0,867	198	0,064	0,939
Diff (%)	-48.784	0	0	0	05.09	-2.089	0	

## 5. CONCLUSIONS

This experimental study concerning the (IT) of AISI D3 steel aims to develop statistical models for predicting the output parameters ( $R_a$ ,  $T^\circ$ ,  $V_B$ ) and optimizing the cutting conditions using the methods (DF and GRA) in order to simultaneously minimize ( $R_a$ ,  $T^\circ$ , and  $V_B$ ). The work carried out leads to the following conclusions:

1. The ANOVA of  $R_a$  demonstrates that ( $f$ ) and ( $r$ ) are significant and strongly impact  $R_a$ , with cont% of 57.86% and 29.63%, respectively. Third in importance is  $V_c$ . ( $T^\circ$ ) ANOVA demonstrates that all input variables are significant ( $P > 0.05$ ). ( $V_c$ ) and ( $a_p$ ) dominate, with cont% of 29.72% and 28.22%, respectively. Third-order factor ( $f$ ) has a cont% of 22.59%, followed by factor ( $r$ ) at 17.98%. The ANOVA of ( $V_B$ ) shows that ( $V_c$ ) and ( $f$ ) are the most significant and dominant variables, with cont% of 66.44% and 25.95%.
2. The proposed mathematical models are precise. The various coefficients of determination ( $R^2$ ) are high. They vary from (96.85%) to (98.51%). These models are operational and industrially useful for the prediction and optimization of parameters ( $R_a$ ,  $T^\circ$ , and  $V_B$ ) in the context of intermittent turning (IT).
3. The application of the optimization method (DF) in (IT), according to very precise cases that meet the industrial requirements, gave us the possibility of choosing the optimal mode, which corresponds to the best solution of optimization envisaged according to:

**1st case:** maximum importance given to ( $R_a$ )  
Optimum speed:  $r = 0.781$  mm,  $V_c = 240.001$  m/min,  $f = 0.08$  mm/rev, and  $a_p = 0.3$  mm.  
Optimized output parameters:  $R_a = 0.825$   $\mu$ m,  $T^\circ = 202.25$  °C and  $V_B = 0.064$  mm.

**2nd case:** maximum importance for ( $R_a$  and  $T^\circ$ )  
Optimal speed:  $r = 0.782$  mm,  $V_c = 240$  m/min,  $f = 0.08$  mm/rev and  $a_p = 0.3$  mm.  
Optimized output parameters:  $R_a = 0.825$   $\mu$ m,  $T^\circ = 202.267$  °C,  $V_B = 0.064$  mm.

**3rd case:** maximum importance for ( $R_a$ ,  $T^\circ$  and  $V_B$ ) simultaneously  
Optimal speed:  $r = 0.781$  mm,  $V_c = 240$  m/min,  $f = 0.08$  mm/rev, and  $a_p = 0.3$  mm.  
Optimized output parameters:  $R_a = 0.825$   $\mu$ m,  $T^\circ = 202.255$  °C,  $V_B = 0.064$  mm.

4. The successful application of the GRA method in (IT) in order to minimize ( $R_a$ ), ( $T^\circ$ ), and ( $V_B$ ) simultaneously, allowed us to find the following optimal regime:  $r = 0.4$  mm,  $V_c = 240$  m/min,  $f = 0.08$  mm/rev and  $a_p = 0.3$  mm.
5. The comparison of the two methods (DF and GRA) for the optimization of the three output parameters together ( $R_a$ ), ( $T^\circ$ ), and ( $V_B$ ), revealed that the two approaches propose the same operating combination for the factors ( $V_c$ ), ( $f$ ), and ( $a_p$ ), with a reduction in tool nose radius ( $r$ ) of 48.78%. This reproduces an increase of 05.09% for the factor ( $R_a$ ) and a decrease of (2.08%) for the factor ( $T^\circ$ ).

This work is by no means exhaustive. It can be extended to the study of other performance parameters such as cutting forces, power consumption, tool vibration, and sound

intensity. Additional research can be conducted to evaluate the performance parameters in hard turning (HT) and in the context (IT) of the lubrication technique (MQL). Finally, the application of other optimization methods such as GA, NSGAI, PSO, GOA, and GWO would lead to better control of the process.

## REFERENCES

- [1] E.M. Rubio, M. Villeta, B. de Agustina, D. Carou, *Surface roughness analysis of magnesium pieces obtained by intermittent turning*, Materials Science Forum, vol. 773-774, pp. 377–391, 2013, doi: [10.4028/www.scientific.net/msf.773-774.377](https://doi.org/10.4028/www.scientific.net/msf.773-774.377)
- [2] H. Persson, M. Agmell, V. Bushlya, J.E. Ståhl, *Experimental and numerical investigation of Burr Formation in intermittent turning of AISI 4140*, Procedia CIRP, vol. 58, pp. 37–42, 2017, doi: [10.1016/j.procir.2017.03.165](https://doi.org/10.1016/j.procir.2017.03.165)
- [3] T.J. Ko, H.S. Kim, *Surface integrity and machineability in intermittent hard turning*, The International Journal of Advanced Manufacturing Technology, vol. 18, pp. 168–175, 2001, doi: [10.1007/s001700170072](https://doi.org/10.1007/s001700170072)
- [4] H.L. Liu, X. Lv, C.Z. Huang, Z.B. Yin, B. Zou, H.T. Zhu, *Tools optimization in efficient intermittent cutting of 2.25Cr1Mo0.25V steel*, Advanced Materials Research, vol. 188, pp. 469–474, 2011, doi: [10.4028/www.scientific.net/amr.188.469](https://doi.org/10.4028/www.scientific.net/amr.188.469)
- [5] H.L. Liu, X. Lv, C.Z. Huang, H.T. Zhu, *Experimental study on intermittent turning 2.25Cr-1mo-0.25V steel with coated cemented carbide tool*, Advanced Materials Research, Vol. 500. Pp. 128–133, 2012, doi: [10.4028/www.scientific.net/amr.500.128](https://doi.org/10.4028/www.scientific.net/amr.500.128)
- [6] D. Carou, E.M. Rubio, C.H. Lauro, J.P. Davim, *The effect of minimum quantity lubrication in the intermittent turning of magnesium based on vibration signals*, Measurement, vol. 94, pp. 338–343, 2016, doi: [10.1016/j.measurement.2016.08.016](https://doi.org/10.1016/j.measurement.2016.08.016)
- [7] F. Gong, J. Zhao, J. Pang, *Evolution of cutting forces and tool failure mechanisms in intermittent turning of hardened steel with Ceramic Tool*, The International Journal of Advanced Manufacturing Technology, vol. 89, pp. 1603–1613, 2016, doi: [10.1007/s00170-016-9178-z](https://doi.org/10.1007/s00170-016-9178-z)
- [8] X. Cui, J. Guo, J. Zheng, *Optimization of geometry parameters for ceramic cutting tools in intermittent turning of hardened steel*, Materials & Design, vol. 92, pp. 424–437, 2016, doi: [10.1016/j.matdes.2015.12.089](https://doi.org/10.1016/j.matdes.2015.12.089)
- [9] E.A. Kudryashov, I.M. Smirnov, E.I. Yatsun, N.A. Khizhnyak, *Stabilizing tool for intermittent turning of complex surfaces*, Russian Engineering Research, vol. 39, pp. 141–146, 2019, doi: [10.3103/s1068798x19020199](https://doi.org/10.3103/s1068798x19020199)
- [10] M. Nayak, R. Sehgal, R. Kumar, *Investigating machinability of Aisi D6 tool steel using CBN tools during hard turning*, Materials Today: Proceedings, vol. 47, pp. 3960–3965, 2021, doi: [10.1016/j.matpr.2021.04.020](https://doi.org/10.1016/j.matpr.2021.04.020)
- [11] M.A. Yallese, J.F. Rigal, K. Chaoui, L. Boulanouar, *The effects of cutting conditions on mixed ceramic and cubic boron nitride tool wear and on surface roughness during machining of X200CR12 steel (60 HRC)*, Proceedings of the Institution of Mechanical Engineers, Part B: Journal of Engineering Manufacture, vol. 219, iss. 1, pp. 35–55, 2005, doi: [10.1243/095440505x8082](https://doi.org/10.1243/095440505x8082)
- [12] H. Bouchelaghem, M.A. Yallese, T. Mabrouki, A. Amirat, J.F. Rigal, *Experimental investigation and performance analyses of CBN insert in hard turning of Cold work tool steel (D3)*, Machining Science and Technology, vol. 14, iss. 4, pp. 471–501, 2010, doi: [10.1080/10910344.2010.533621](https://doi.org/10.1080/10910344.2010.533621)
- [13] M. Nouioua, M.A. Yallese, R. Khettabi, S. Belhadi, T. Mabrouki, *Comparative assessment of cooling conditions, including MQL technology on machining factors in an environmentally friendly approach*, The International Journal of Advanced Manufacturing Technology, vol. 91, pp. 3079–3094, 2017, doi: [10.1007/s00170-016-9958-5](https://doi.org/10.1007/s00170-016-9958-5)
- [14] D.H. Lee, I.J. Jeong, K.J. Kim, *A desirability function method for optimizing mean and variability of multiple responses using a posterior preference articulation approach*, Quality and Reliability Engineering International, vol. 34, iss. 3, pp. 360–376, 2018, doi: [10.1002/qre.2258](https://doi.org/10.1002/qre.2258)
- [15] K. Safi, M.A. Yallese, S. Belhadi, T. Mabrouki, S. Chihaoui, *Parametric study and multi-criteria optimization during turning of x210cr12 steel using the desirability function and Hybrid Taguchi-WASPAS method*, Proceedings of the Institution of Mechanical Engineers, Part C: Journal of Mechanical Engineering Science, vol. 236, iss. 15, pp. 8401–8420, 2022, doi: [10.1177/09544062221086171](https://doi.org/10.1177/09544062221086171)
- [16] V.R. Balwan, B.M. Dabade, B.B. Kabnure, *Optimization of surface finish and material removal rate while turning hardened en 353 steel using GRA*, Materials Today: Proceedings, vol. 59, pp. 331–338, 2022, doi: [10.1016/j.matpr.2021.11.183](https://doi.org/10.1016/j.matpr.2021.11.183)

- [17] L. Al-Durgham, W.H. AlAlaween, N.T. Albashabsheh, *Optimizing the turning operation via using the Grey Relational Grade*, International Journal of Mechanical Engineering and Robotics Research, vol. 11, no. 6, pp. 452–459, 2022, doi: [10.18178/ijmerr.11.6.452-459](https://doi.org/10.18178/ijmerr.11.6.452-459)
- [18] P. Darandale, G.N. Kadam, *Influence of tool nose radius on surface roughness of ss304 using optimization technique*, International Research Journal of Modernization in Engineering Technology and Science, vol. 4, iss. 5, pp. 1893-1899, 2022.
- [19] D. Carou, E.M. Rubio, C.H. Lauro, J.P. Davim, *Experimental investigation on surface finish during intermittent turning of uns m11917 magnesium alloy under dry and near dry machining conditions*, Measurement, vol. 56, pp. 136–154, 2014, doi: [10.1016/j.measurement.2014.06.020](https://doi.org/10.1016/j.measurement.2014.06.020)
- [20] E.O. Ezugwu, C.I. Okeke, *Tool life and wear mechanisms of tin coated tools in an intermittent cutting operation*, Journal of Materials Processing Technology, vol. 116, iss. 1, pp. 10–15, 2001, doi: [10.1016/s0924-0136\(01\)00852-4](https://doi.org/10.1016/s0924-0136(01)00852-4)
- [21] E. García-Martínez, V. Miguel, A. Martínez-Martínez, J. Coello, J.A. Naranjo, M.C. Manjabacas, *Optimization of the dry turning process of  $Ti_{48}Al_2Cr_2Nb$  aluminide based on the cutting tool configuration*, Materials, vol. 15, iss. 4, pp. 1–18, 2022, doi: [10.3390/ma15041472](https://doi.org/10.3390/ma15041472)
- [22] K. Safi, M.A. Yallese, S. Belhadi, T. Mabrouki, A. laouissi, *Tool wear, 3D surface topography, and comparative analysis of GRA, Moora, dear, and WASPAS optimization techniques in turning of Cold work tool steel*, The International Journal of Advanced Manufacturing Technology, vol. 121, pp. 701–721, 2022, doi: [10.1007/s00170-022-09326-6](https://doi.org/10.1007/s00170-022-09326-6)
- [23] Y.H. Zhou, J. Zhao, X.B. Cui, *Cutting performance and tool failure in intermittent turning processes of an  $Al_2O_3$ -based micro-nano-composite ceramic tool*, Materials Science Forum, vol. 723, pp. 56–61, 2012, doi: [10.4028/www.scientific.net/msf.723.56](https://doi.org/10.4028/www.scientific.net/msf.723.56)
- [24] H. Aouici, M.A. Yallese, B. Fnides, T. Mabrouki, *Machinability investigation in hard turning of AISI H11 hot work steel with CBN tool*, Mechanics, Vol. 86,no.6, pp. 71-77, 2010.
- [25] O. Zerti, M.A. Yallese, R. Khettabi, K. Chaoui, T. Mabrouki, *Design optimization for minimum technological parameters when dry turning of AISI D3 steel using Taguchi method*, The International Journal of Advanced Manufacturing Technology, vol. 89,pp 1915–1934, 2017, doi: [10.1007/s00170-016-9162-7](https://doi.org/10.1007/s00170-016-9162-7)
- [26] S.A. Bagaber, A.R. Yusoff, *Multi-objective optimization of cutting parameters to minimize power consumption in dry turning of stainless steel 316*, Journal of Cleaner Production, vol. 157, pp. 30–46, 2017, doi: [10.1016/j.jclepro.2017.03.231](https://doi.org/10.1016/j.jclepro.2017.03.231)
- [27] A. Perec, *Desirability function analysis (DFA) in multiple responses optimization of abrasive water jet cutting process*, Reports in Mechanical Engineering, vol. 3, no. 1, pp. 11–19, 2022, doi: [10.31181/rme200103011p](https://doi.org/10.31181/rme200103011p)
- [28] S. Boucherit, S. Berkani, M. A. Yallese, A. Haddad, S.Belhadi, *Dry turning of X2CrNi18-09 using coated carbide tools: modelling and optimization of multiple performance characteristics*, Mechanics, vol. 25, pp 487-500, 2019, doi: [10.5755/j01.mech.25.6.22367](https://doi.org/10.5755/j01.mech.25.6.22367)
- [29] I. Kouahla, M.A. Yallese, S. Belhadi, K. Safi, M. Nouioua, *Tool vibration, surface roughness, cutting power, and productivity assessment using RSM and GRA approach during machining of Inconel 718 with PVD-coated carbide tool*, The International Journal of Advanced Manufacturing Technology, vol. 122, pp. 1835–1856, 2022, doi: [10.1007/s00170-022-09988-2](https://doi.org/10.1007/s00170-022-09988-2)
- [30] D. Mukherjee, R. Ranjan, S.C. Moi, *Multi-response optimization of surface roughness and MRR in turning using Taguchi Grey Relational Analysis (TGRA)*, International Research Journal of Multidisciplinary Scope, vol. 3, iss. 2, pp. 01–07, 2022, doi: [10.47857/irjms.2022.v03i02.068](https://doi.org/10.47857/irjms.2022.v03i02.068)